Acta Crystallographica Section D
**Biological Crystallography**
ISSN 0907-4449

# Phosphorylation adjacent to the nuclear localization signal of human dUTPase abolishes nuclear import: structural and mechanistic insights

**Gergely Róna,[a]* Mary Marfori,[b] Máté Borsos,[a] Ildikó Scheer,[a] Enikő Takács,[a] Judit Tóth,[a] Fruzsina Babos,[c] Anna Magyar,[c] Anna Erdei,[d] Zoltán Bozóky,[a] László Buday,[a] Bostjan Kobe[b] and Beáta G. Vértessy[a,e]***

[a]Institute of Enzymology, RCNS, Hungarian Academy of Sciences, 1113 Budapest, Hungary, [b]School of Chemistry and Molecular Biosciences, Institute for Molecular Bioscience and Australian Infectious Diseases Research Centre, The University of Queensland, Brisbane, Queensland 4072, Australia, [c]Department of Organic Chemistry, University Eötvös Loránd, 1117 Budapest, Hungary, [d]Department of Immunology, University Eötvös Loránd, 1117 Budapest, Hungary, and [e]Department of Applied Biotechnology, Budapest University of Technology and Economics, 1111 Budapest, Hungary

Correspondence e-mail: rona@enzim.hu, vertessy@mail.bme.hu, vertessy@ttk.mta.hu

Received 28 June 2013
Accepted 19 August 2013

**PDB References:** importin-α–dUTPase NLS complex, 4mz5; importin-α–dUTPase S11E mutant NLS complex, 4mz6

Phosphorylation adjacent to nuclear localization signals (NLSs) is involved in the regulation of nucleocytoplasmic transport. The nuclear isoform of human dUTPase, an enzyme that is essential for genomic integrity, has been shown to be phosphorylated on a serine residue (Ser11) in the vicinity of its nuclear localization signal; however, the effect of this phosphorylation is not yet known. To investigate this issue, an integrated set of structural, molecular and cell biological methods were employed. It is shown that NLS-adjacent phosphorylation of dUTPase occurs during the M phase of the cell cycle. Comparison of the cellular distribution of wild-type dUTPase with those of hyperphosphorylation- and hypophosphorylation-mimicking mutants suggests that phosphorylation at Ser11 leads to the exclusion of dUTPase from the nucleus. Isothermal titration microcalorimetry and additional independent biophysical techniques show that the interaction between dUTPase and importin-α, the karyopherin molecule responsible for 'classical' NLS binding, is weakened significantly in the case of the S11E hyperphosphorylation-mimicking mutant. The structures of the importin-α–wild-type and the importin-α–hyperphosphorylation-mimicking dUTPase NLS complexes provide structural insights into the molecular details of this regulation. The data indicate that the post-translational modification of dUTPase during the cell cycle may modulate the nuclear availability of this enzyme.

## 1. Introduction

The distribution of proteins within eukaryotic cells requires specific transport processes, particularly for larger proteins. Nucleocytoplasmic trafficking is facilitated by karyopherins (Görlich *et al.*, 1995). Importin-α and importin-β transporters are involved in the nuclear import of many cargo proteins possessing 'classical' nuclear localization signals (NLSs). The linear motif NLSs comprise 5–15 amino-acid residues that attach cargo proteins to karyopherins. Classical NLSs have one (monopartite) or two (bipartite) clusters of basic residues binding to one or both (minor and major) NLS-binding sites on the importin-α adaptor (Lange *et al.*, 2007; Marfori *et al.*, 2011). For several NLSs, the interaction with importin-α has been characterized structurally, with the most important importin-α-binding positions on the NLS being designated P1–P6 (bound in the major NLS-binding site) and P1′–P4′ (bound in the minor NLS-binding site) (Marfori *et al.*, 2011).

Nucleocytoplasmic trafficking is under multi-level regulatory control to orchestrate cellular events. For instance,

**Table 1**
Predicted binding to the major binding site of importin-$\alpha$ by proteins reported in the literature to be phosphorylated in the vicinity of their NLSs (phosphorylated residues are shown in italics).

| | NLS binding to major binding site of importin-$\alpha$ | | | | | | | | | | |
|---|---|---|---|---|---|---|---|---|---|---|---|
| | P−2 | P−1 | P0 | P1 | P2 | P3 | P4 | P5 | P6 | Kinase | References |
| SV40 TAg | Ser123 | *Thr* | Pro | Lys | Lys | Lys | Arg | Lys | Val | Cdk1–Cdc28 | Harreman *et al.* (2004), Jans *et al.* (1991) |
| Swi6 | Gly159 | *Ser* | Pro | Leu | Lys | Lys | Leu | Lys | Ile | | Harreman *et al.* (2004), Geymonat *et al.* (2004), Sidorova *et al.* (1995), Kosugi *et al.* (2009) |
| Swi5 | Arg645 | *Ser* | Pro | Arg | Lys | Arg | Gly | Arg | Pro | | Jans *et al.* (1995), Moll *et al.* (1991), Kosugi *et al.* (2009) |
| Cdh1 | Ser42 | *Ser* | Pro | Ser | Arg | Arg | Ser | Arg | Prp | | Kosugi *et al.* (2009), Jaquenoud *et al.* (2002) |
| Fzr1 | Arg162 | *Ser* | Pro | Arg | Lys | Pro | Thr | Arg | Lys | | Zhou *et al.* (2003), Huynh *et al.* (2009) |
| Mcm3 | Lys764 | *Ser* | Pro | Lys | Lys | Arg | Gln | Lys | Val | | Liku *et al.* (2005) |
| Acm1 | Arg30 | *Ser* | Pro | Ser | Lys | Arg | Arg | Ser | Gln | | Enquist-Newman *et al.* (2008), Kosugi *et al.* (2009) |
| Msa1 | Pro53 | *Ser* | Pro | Asn | Lys | Arg | Arg | Leu | Ser | | Kosugi *et al.* (2009) |
| Psy4 | Glu319 | *Thr* | Pro | Arg | Lys | Arg | Lys | Pro | Thr | | Kosugi *et al.* (2009) |
| Pds1 | Val70 | *Ser* | Pro | Thr | Lys | Arg | Leu | His | Thr | | Kosugi *et al.* (2009) |
| Yen1 | Ile678 | *Ser* | Pro | Ile | Lys | Lys | Ser | Arg | Thr | | Kosugi *et al.* (2009) |
| Lmnb2 | Ser411 | *Ser* | Arg | Gly | Lys | Arg | Arg | Arg | Ile | PKC | Hennekes *et al.* (1993) |
| AhR | Ty10 | Ala | *Ser* | Arg | Lys | Arg | Arg | Lys | Pro | | Ikuta *et al.* (2004) |
| v-Jun | Ser246 | Lys | *Ser* | Arg | Lys | Arg | Lys | Leu | Arg | | Tagawa *et al.* (1995) |

phosphorylation adjacent to NLSs can modulate (either inhibit or enhance) nucleocytoplasmic trafficking in several cases (Table 1 and references therein; Fontes, Teh, Toth *et al.*, 2003; Jans & Hübner, 1996; Kaffman *et al.*, 1998; Kosugi *et al.*, 2009; Nardozzi *et al.*, 2010; Poon & Jans, 2005). Phosphorylation by cell-cycle-dependent kinases (*e.g.* cyclin-dependent protein kinase 1; Cdk1) regulates processes within the G2 and M phases and at the onset of the G1 phase. Although Cdk1-dependent phosphorylation in the vicinity of NLSs has also been reported for many other cargo proteins of key significance in genomic integrity, such as p53 (Lee *et al.*, 2010), UBA E1 (Stephen *et al.*, 1997), UNG2 (Hagen *et al.*, 2008) and dUTPase (Tinkelenberg *et al.*, 2003), it was concluded that these phosphorylation events did not affect nucleocytoplasmic trafficking. This controversy may result from a lack of the use of relevant hyperphosphorylation-mimicking mutants in some cases. Therefore, a coherent view of the cross-talk between phosphorylation and trafficking is not yet available. Also, the exact structural and molecular details of phosphorylation-driven regulation in the NLS vicinity need to be addressed.

Our aim was to investigate whether phosphorylation of the nuclear isoform of human dUTPase, an enzyme essential for genome integrity (Mol *et al.*, 1996; Vértessy & Tóth, 2009), has any effect on its nucleocytoplasmic trafficking, despite an earlier study that concluded that it does not (Tinkelenberg *et al.*, 2003). The enzymes of the dUTPase family play an important role both in genome integrity and in *de novo* thymidylate biosynthesis. dUTPases catalyze the pyrophosphorolysis of dUTP into dUMP and inorganic pyrophosphate, thereby lowering the cellular dUTP level and preventing the incorporation of dUMP moieties (uracil) into DNA (Vértessy & Tóth, 2009; Galperin *et al.*, 2006). The produced dUMP is methylated on the pyrimidine ring by thymidylate synthase to form dTMP, which is then phosphorylated to dTTP. A lack or inhibition of dUTPase within the cell leads to major perturbations of the dUTP/dTTP levels and increases the uracil content of DNA. The repair of highly uracil-substituted DNA at high cellular dUTP levels leads to hyperactive futile cycles, DNA breaks and cell death (Duncan & Weiss, 1982; Gadsden *et al.*, 1993; Koehler & Ladner, 2004; Pecsi *et al.*, 2012; Muha *et al.*, 2012; Merényi *et al.*, 2011).

In most eukaryotes, dUTPases have two isoforms, one of which is nuclear and the other of which is either cytoplasmic (in *Drosophila*) or mitochondrial (*e.g.* in human cells) (Ladner & Caradonna, 1997; Ladner, McNulty *et al.*, 1996; Vértessy & Tóth, 2009; Muha *et al.*, 2009; Békési *et al.*, 2004). In human cells, the expression patterns of the two isoforms are different: the mitochondrial isoform is constitutively expressed, whereas the nuclear isoform is under cell-cycle control (Ladner & Caradonna, 1997; Ladner, McNulty *et al.*, 1996). The mature mitochondrial isoform is created by post-translational cleavage to remove the mitochondrial leader sequence upon import into the mitochondrion (Supplementary Fig. S1[1]). With the exception of a short N-terminal segment, the mature mitochondrial and nuclear isoforms are identical. Interestingly, the mitochondrial isoform also contains the NLS sequence, albeit sequestered away from the cognate karyopherins. The first three-dimensional structure of human dUTPase was determined using an N-terminally truncated construct lacking the NLS and some additional residues (Mol *et al.*, 1996). Further detailed structural studies of the full-length nuclear isoform of human dUTPase could not locate the N-terminal segment (approximately 20 residues) using X-ray crystallography (Varga *et al.*, 2007), presumably owing to its high flexibility. However, the orientation and molecular shape of this segment could be probed using small-angle X-ray scattering (Takács *et al.*, 2009). Based on the conserved general presence of the NLS segment in eukaryotes, the nuclear availability of dUTPase activity in eukaryotes seems to be important for cellular function, although this hypothesis has

[1] Supplementary material has been deposited in the IUCr electronic archive (Reference: DW5062). Services for accessing this material are described at the back of the journal.

yet to be tested experimentally. In this respect, it needs to be mentioned that nuclear localization of other enzymes of thymidylate biosynthesis has recently been shown to be crucial to prevent the incorporation of uracil into DNA (MacFarlane *et al.*, 2011).

In the present work, we focused on the potential role of NLS-adjacent phosphorylation of dUTPase in nucleocytoplasmic trafficking. We found that phosphorylation occurs in the M phase. Constructing and testing hyperphosphorylation-mimicking (hyper-P) and hypophosphorylation-mimicking (hypo-P) mutants in parallel to the wild-type (WT) protein, we found that Cdk1-dependent phosphorylation of dUTPase results in exclusion of the protein from the nucleus. We then set out to characterize the structural basis of inhibition of nuclear transport through NLS-adjacent phosphorylation *via* biophysical techniques in the solution phase and by the determination of the three-dimensional structures of dUTPase NLS–importin-$\alpha$ complexes. Our data provide a molecular explanation for understanding the process by which phosphorylation impedes the nuclear import of dUTPase.

## 2. Materials and methods

### 2.1. Cell culture and cloning of constructs

293T HEK (human embryonic kidney) cells were kindly provided by Professor Yvonne Jones (Cancer Research UK, Oxford, England). Other cell lines were purchased from ATCC. The cells were cultured in DMEM/F12 HAM (Sigma) supplemented with penicillin–streptomycin solution (50 µg ml$^{-1}$; Gibco) and 10% FBS (Gibco), except for the NIH3T3 cells, where 10% NBS was applied. Human dUTPase nuclear isoform (hDUT) was amplified from an expression vector previously described in Varga *et al.* (2007) and cloned into the *Xho*I/*Kpn*I restriction sites in-frame with DsRed-Monomer (with dutN1F and dutN1R oligos) in the pDsRed-M-N1 vector (Clontech), yielding the fusion construct termed DsR-DUT. Site-directed mutagenesis was performed by the QuikChange method (Stratagene). The primers used for cloning and mutagenesis were synthesized by Eurofins MWG GmbH and are summarized in Supplementary Table S1. All constructs were verified by sequencing at Eurofins MWG GmbH.

### 2.2. Fluorescence imaging and analysis of DsRed-tagged constructs

For DNA transfections, FuGENE HD (Roche) was used according to the manufacturer's instructions. Briefly, subconfluent cultures of different cell lines grown in 24-well plates were incubated with 0.5 µg DNA together with 2 µl FuGENE HD reagent in serum-containing medium for 24 h. Images were acquired using either a confocal microscope (Zeiss LSM 710) or a widefield microscope (Leica DM IL LED Fluo) equipped with a Leica DFC345 FX monochrome camera.

### 2.3. Immunofluorescence microscopy

The phosphorylation of endogenous dUTPase and its cell-cycle dependency were investigated by immunofluorescence microscopy. Cells were grown on glass cover slips, fixed with 4% paraformaldehyde, permeabilized with 0.1% Triton X-100 in PBS for 10 min and blocked with 5% goat serum, 1% BSA in PBS for 2 h. Samples were incubated with primary antibodies overnight at 277 K in blocking buffer. After extensive washing steps, cells were incubated with secondary antibodies (1:1000) coupled to either Rhodamine Red-X or Alexa 488 (Molecular Probes), stained with 1 µg ml$^{-1}$ DAPI and finally embedded in FluorSave Reagent (Calbiochem). The following antibodies were used to detect the proteins in immunofluorescence: anti-hDUT, a previously described antibody raised against recombinant full-length nonphosphorylated dUTPase that recognizes both nonphosphorylated and phosphorylated dUTPase (dilution used 1:2000; Bozóky *et al.*, 2011; Merényi *et al.*, 2011), and anti-histone-H3 (phospho-S10) (dilution used 1:2000, ab14955, Abcam). A polyclonal antibody generated against the phosphorylated dUTPase NLS peptide (EETPAI/pSer/PSKRAC; anti-S11P-hDUT) was custom-produced and affinity-purified by GenScript (Piscataway, USA) and was used at a 1:100 dilution. This antibody only recognizes phosphorylated human dUTPase.

### 2.4. Recombinant protein production

The dUTPase constructs were expressed in *Escherichia coli* Rosetta BL21 (DE3) pLysS strain and were purified using Ni–NTA affinity resin (Qiagen) (Pecsi *et al.*, 2010; Pécsi *et al.*, 2011; Varga *et al.*, 2007; Tóth *et al.*, 2007). Transformed cells grown in Luria broth medium were induced at an $A_{600\ nm}$ of 0.6 with 0.5 m*M* isopropyl $\beta$-D-1-thiogalactopyranoside (IPTG) for 4 h at 303 K. Cells were harvested and lysed in lysis buffer [50 m*M* Tris–HCl pH 8.0, 300 m*M* NaCl, 0.5 m*M* EDTA, 0.1% Triton X-100, 10 m*M* $\beta$-mercaptoethanol, 1 m*M* phenylmethylsulfonyl fluoride, 5 m*M* benzamidine and a cOmplete EDTA-free protease-inhibitor cocktail tablet (Roche)] assisted by sonication and the cell debris was pelleted by centrifugation at 20 000*g* for 30 min at 277 K. The supernatant was applied onto an Ni–NTA column and washed with lysis buffer containing 50 m*M* imidazole. The dUTPase was finally eluted with elution buffer (50 m*M* HEPES pH 7.5, 30 m*M* KCl, 500 m*M* imidazole, 10 m*M* $\beta$-mercaptoethanol). For both the different dUTPase constructs and importin-$\alpha$, further purification was achieved by gel filtration on a Superdex 200 HR column (GE Healthcare) in 20 m*M* Tris–HCl pH 8.0, 125 m*M* NaCl, 1 m*M* $MgCl_2$, 2 m*M* dithiothreitol (DTT). The proteins were >95% pure as assessed by SDS–PAGE.

N-terminally truncated mouse importin-$\alpha$2 (NP_034785) lacking 69 N-terminal residues (residues 70–529; abbreviated as importin-$\alpha$ $\Delta$IBB in the present study) was expressed recombinantly and purified as described in Fontes *et al.* (2000). Protein concentrations correspond to subunits throughout this study.

**Table 2**
Data obtained from CD and ITC measurements.

| | DUT | DUT-S11E | DUT-S11Q |
|---|---|---|---|
| CD measurements, $T_m$ values detected† (K) | | | |
| dUTPase | 331.5 ± 1.6 | 331.4 ± 0.1 | 330.6 ± 1.3 |
| Importin-$\alpha$ | 308.8 ± 1.5 | 308.8 ± 1.5 | 308.8 ± 1.5 |
| dUTPase + importin-$\alpha$ | 329.5 ± 0.6/ 316.7 ± 1.6 | 330.5 ± 2.0/ 309.8 ± 0.2 | 329.6 ± 0.3/ 317.5 ± 1.1 |
| ITC measurements‡ | | | |
| $N$ (molar binding ratio) | 0.74 ± 0.02 | 0.73 ± 0.03 | 0.71 ± 0.01 |
| $K_d$ ($\mu M$) | 0.79 ± 0.26 | 9.62 ± 1.54 | 0.76 ± 0.15 |
| $\Delta H$ (kcal mol$^{-1}$) | −22.84 ± 0.90 | −20.31 ± 1.31 | −23.78 ± 0.56 |
| $\Delta S$ (cal mol$^{-1}$ K$^{-1}$) | −50.0 | −46.3 | −53.1 |

† Values (± standard deviation) extracted from independent experiments. ‡ The reliabilities of the fits are shown by the error values. 1 cal = 4.184 J.

### 2.5. Analytical gel filtration and native PAGE analysis

Analytical gel filtration was conducted on a Superdex 200 HR column (GE Healthcare). Samples were applied in a total volume of 500 µl at a concentration of 25 µ*M* for both importin-$\alpha$ and dUTPase. Gel filtration of the complexes was carried out after co-incubation at room temperature for 15 min. Fractionation was started at identical elution volumes for all samples; 0.5 ml fractions were collected and analyzed on SDS–PAGE. Native PAGE analysis was performed according to the instructions of the manufacturer of the Mini-PROTEAN 3 cell system (Bio-Rad) using a discontinuous buffer system consisting of a 4% stacking gel (pH 7.8) and a 10% resolving gel (pH 9.0).

### 2.6. Isothermal titration microcalorimetry (ITC)

ITC experiments were carried out at 293 K on a MicroCal iTC$_{200}$ instrument following previously described protocols (Nagy *et al.*, 2013; Kovári *et al.*, 2008; Németh-Pongrácz *et al.*, 2007). Proteins were dialyzed into 20 m*M* HEPES pH 7.5, 100 m*M* NaCl, 5 m*M* MgCl$_2$, 10 m*M* $\beta$-mercaptoethanol and were used at concentrations of 45 µ*M* importin-$\alpha$ (in the cell) and 460 µ*M* dUTPase (in the syringe). Aliquots of 2 µl were used for at least ten injection steps (except for the first step of 0.5 µl, which was not considered in the analysis). As a control, dUTPase was also injected into the buffer to allow mixing and dilution heat effects to be considered. Data analysis was performed using the *Origin* 7.5 software (MicroCal). The binding isotherms were fitted with a 'one set of sites' independent binding sites model. The values extracted are shown in Table 2.

### 2.7. Circular-dichroism measurements

Circular-dichroism (CD) spectra were recorded on a Jasco 720 spectropolarimeter using a 1 mm path-length thermostatted cuvette. Thermal unfolding measurements were performed in phosphate buffer (100 m*M* phosphate, 2 m*M* MgCl$_2$ pH 7.5) using 5 µ*M* importin-$\alpha$ or 5 µ*M* dUTPase or a mixture of the two proteins. The temperature was increased by 1 K min$^{-1}$ between 288 and 343 K and the CD signal was monitored at 210 nm. The fraction of the folded protein was calculated using a previously reported method (Takács *et al.*, 2004) and was plotted against temperature to give unfolding curves. Briefly, data were fitted to the equation $f_D = [\theta - (\theta_N + s_N T)]/[(\theta_D + s_D T) - (\theta_N + s_N T)]$, where $f_D$ is the denaturated protein fraction, $\theta$ is an optical property measured at the given temperature ($T$), $\theta_D$ and $\theta_N$ are the intersections of the fitted linear slopes of the measured values for totally unfolded or native protein, respectively, and $s_D$ and $s_N$ are the fitted linear slopes of the measured values for totally unfolded or native protein, respectively. $T_m$ was determined as the inflection point of the $f_D(T)$ function from parallel experiments (Table 2). Functions were plotted using *Origin* 7.0 (MicroCal).

**Table 3**
Crystallographic data-collection and refinement statistics.

Values in parentheses are for the highest resolution shell.

| | dUTPase NLS WT | dUTPase S11E mutant |
|---|---|---|
| PDB code | 4mz5 | 4mz6 |
| Data collection | | |
| Space group | $P2_12_12_1$ | $P2_12_12_1$ |
| Unit-cell parameters (Å) | $a$ = 77.88, $b$ = 89.99, $c$ = 99.73 | $a$ = 78.03, $b$ = 89.95, $c$ = 99.44 |
| Resolution (Å) | 99.73–2.10 (2.21–2.10) | 99.44–1.88 (1.98–1.88) |
| Total No. of reflections | 238847 (34586) | 421273 (61134) |
| No. of unique reflections | 41431 (5965) | 57564 (8321) |
| Multiplicity | 5.8 (5.8) | 7.3 (7.3) |
| Completeness (%) | 99.4 (100.0) | 99.9 (100.0) |
| $\langle I/\sigma(I)\rangle$ | 10.8 (2.3) | 25.8 (2.4) |
| $R_{merge}$† | 0.101 (0.794) | 0.049 (0.806) |
| Refinement | | |
| No. of importin-$\alpha$ molecules in the asymmetric unit | 1 | 1 |
| No. of peptide molecules in the asymmetric unit | 2 | 2 |
| No. of protein atoms | 3244 | 3252 |
| No. of dUTPase peptide atoms | 150 | 141 |
| No. of waters | 192 | 336 |
| $R_{cryst}/R_{free}$‡ (%) | 19.9/23.2 | 17.4/19.5 |
| Luzzati plot coordinate error (Å) | 0.292 | 0.228 |
| Average $B$ factors (Å$^2$) | | |
| Wilson $B$ factor | 34.48 | 31.53 |
| Protein | 49.5 | 38.9 |
| Peptide | 59.9 | 50.9 |
| Water | 48.0 | 44.5 |
| R.m.s. deviations from ideal values | | |
| Bond lengths (Å) | 0.006 | 0.015 |
| Bond angles (°) | 1.034 | 1.496 |
| Ramachandran plot§, residues in (%) | | |
| Favoured region | 98.9 | 98.6 |
| Allowed region | 1.1 | 1.4 |
| Disallowed region | 0.0 | 0.0 |

† $R_{merge} = \sum_{hkl}\sum_i |I_i(hkl) - \langle I(hkl)\rangle|/\sum_{hkl}\sum_i I_i(hkl)$, where $I_i(hkl)$ is the intensity of an individual measurement of the reflection with Miller indices $hkl$ and $\langle I(hkl)\rangle$ is the mean intensity of that reflection. Calculated for $I > -3\sigma(I)$. ‡ $R_{work} = \sum_{hkl}||F_{obs}| - |F_{calc}||/\sum_{hkl}|F_{obs}|$, where $|F_{obs}|$ and $|F_{calc}|$ are the observed and calculated structure-factor amplitudes, respectively. $R_{free}$ is equivalent to $R_{work}$ but calculated using reflections (5%) that were omitted from the refinement process. § Calculated using *MolProbity* (Chen *et al.*, 2010).

### 2.8. Peptide synthesis

Peptides corresponding to wild-type dUTPase NLS and the dUTPase NLS S11E mutant (for a list of the peptides used in the present study, see Supplementary Table S1) were synthesized by solid-phase peptide synthesis using the Fmoc/tBu

strategy (SYRO automated synthesizer, MultiSynTech) on Rink-Amide MBHA resin with the double-coupling protocol using 1,3-diisopropylcarbodiimide (DIC) and 1-hydroxybenzotriazole (HOBt) as coupling reagents. The crude products were purified by semipreparative RP-HPLC and the purified compounds were characterized by analytical HPLC (Knauer system using a Phenomenex Jupiter C18 column) and mass spectrometry (Esquire 3000+ ion-trap mass spectrometer, Bruker Daltonics).

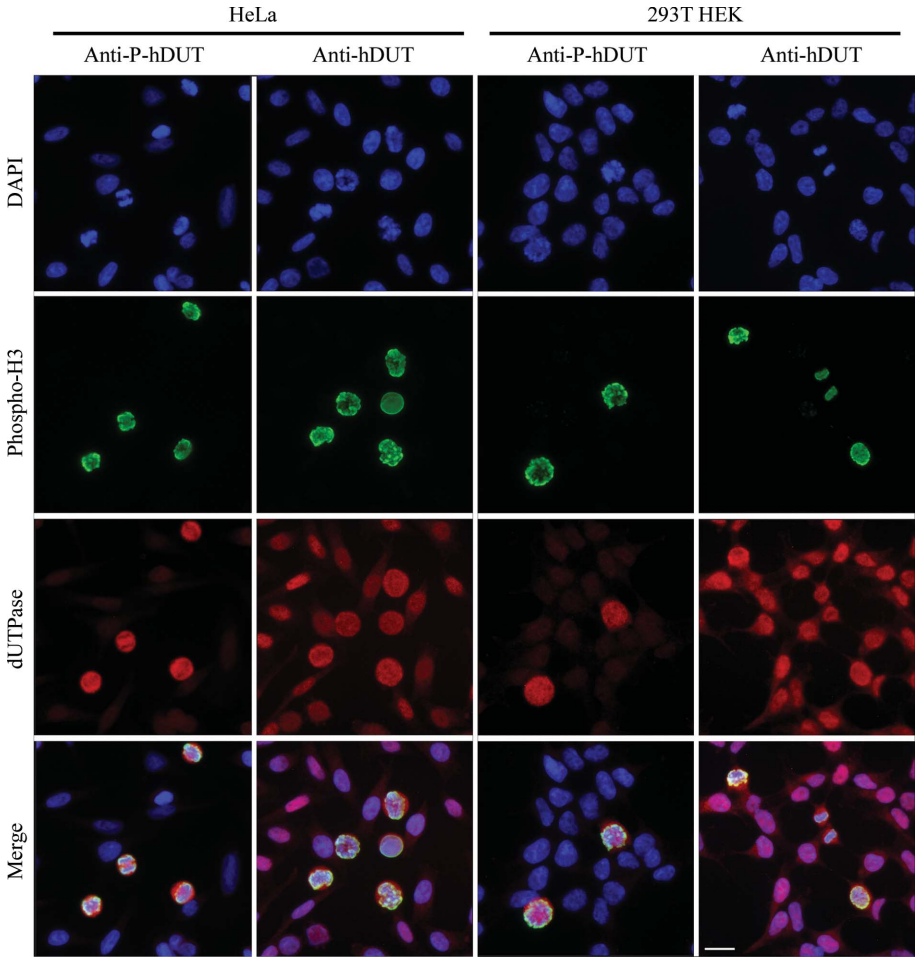


**Figure 1**
Cell-cycle-dependent phosphorylation of dUTPase in asynchronous cells. Asynchronous 293T and HeLa cells were stained against dUTPase (anti-hDUT) and the phosphorylated NLS segment of dUTPase (anti-P-hDUT). Immunofluorescence shows that dUTPase phosphorylation coincides with an M-phase marker [anti-histone-H3 (phospho-S10)]. The cell nucleus was stained with DAPI. The scale bar represents 20 µm.

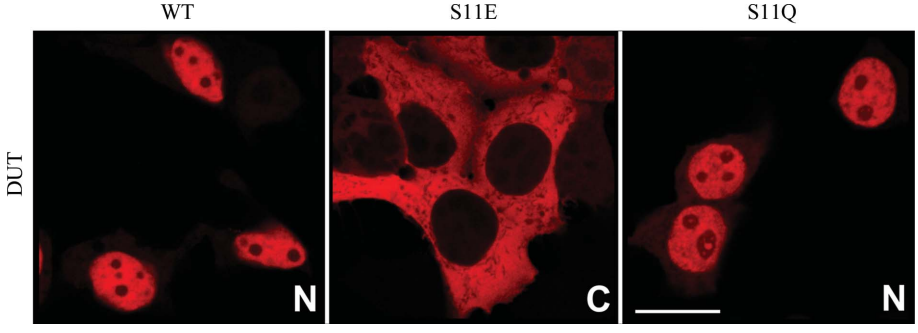


**Figure 2**
Phosphorylation-dependent cellular localization patterns of dUTPase. 293T cells transiently expressing DsRed-fused WT, S11E and S11Q dUTPases were visualized. The WT construct and the S11Q (hypophosphorylation-mimicking) mutant are mainly nuclear, while the S11E (hyperphosphorylation-mimicking) mutant is clearly excluded from the cell nucleus. The scale bar represents 20 µm.

### 2.9. Crystallization and X-ray crystallography

Crystals of mouse importin-$\alpha$ $\Delta$IBB–dUTPase NLS peptide complexes were obtained under conditions similar to those used to obtain the previously determined importin-$\alpha$ $\Delta$IBB–NLS complexes (Fontes, Teh, Jans *et al.*, 2003, Fontes *et al.*, 2000). The peptides AISPSKRARPAEV and AI**E**PSKRARPAEV were used as the wild-type and S11E mutant (the mutation is shown in bold) dUTPase NLS sequences. Importin-$\alpha$ $\Delta$IBB was concentrated to 15–20 mg ml$^{-1}$ using Centricon-30 (Millipore) and stored at 253 K. The crystals were obtained by co-crystallization by combining 1 µl protein solution, 0.5 µl peptide solution (peptide:protein molar ratio of 3.5) and 1 µl reservoir solution on a cover slip and suspending it over 0.5 ml reservoir solution. Single crystals were obtained using a reservoir solution consisting of 0.65–0.70 *M* sodium citrate pH 6.0, 10 m*M* dithiothreitol after 15–20 d.

Single crystals were cryoprotected in reservoir solution supplemented with 25% glycerol and data were collected on the Australian Synchrotron MX1 beamline using the *Blu-Ice* software (McPhillips *et al.*, 2002). Data were processed using *XDS* (Kabsch, 2010) and *SCALA* (Winn *et al.*, 2011; Cowtan *et al.*, 2011) and molecular replacement was performed by *Phaser* (McCoy *et al.*, 2007) using an importin-$\alpha$ $\Delta$IBB structure (PDB entry 3ukw; NLS coordinates removed; Marfori *et al.*, 2012) as a model. Clear difference density was observed in the NLS binding site of importin-$\alpha$ $\Delta$IBB and the dUTPase NLS side chains could be unambiguously assigned. The dUTPase peptide backbone was manually built in *Coot* (Emsley & Cowtan, 2004). Iterative cycles of refinement (*PHENIX*; Adams *et al.*, 2010) and model building (*Coot*)

gave final models with good geometry (Table 3). Data were deposited in the PDB as entries 4mz5 and 4mz6 for the complexes of importin-$\alpha$ $\Delta$IBB with wild-type and mutant dUTPase NLS segments, respectively.

## 3. Results and discussion

### 3.1. The effect of phosphorylation on dUTPase nuclear trafficking during the cell cycle

The nuclear isoform of human dUTPase was suggested to be phosphorylated by the kinase Cdk1 in the vicinity of its NLS (Ser11; Tinkelenberg *et al.*, 2003; Ladner, Carr *et al.*, 1996). Cdk1–cyclin B has been reported to become activated in the M phase of the cell cycle. Therefore, we investigated the putative cell-cycle dependence of the phosphorylation of the endogenous dUTPase using an M-phase marker [anti-histone-H3 (phospho-S10) antibody], anti-hDUT antibody and our anti-S11P-hDUT antibody in parallel. We observe that the anti-hDUT antibody stains all cells in an asynchronous cell population, whereas the anti-S11P-hDUT antibody (generated against the phosphorylated NLS segment of the dUTPase) only stains cells in the M phase (Fig. 1). Based on these results, we conclude that phosphorylation of dUTPase occurs within the nucleus and is scheduled at the M phase of the cell cycle. Thus, our results further argue in favour of the potential involvement of the Cdk1 kinase and its partner cyclin B in this process.

Next, we aimed to determine whether there are any functional effects associated with the phosphorylation of dUTPase. Towards this aim, we decided to utilize different point mutations at the Ser11 phosphorylation site. Glutamic acid mimics a constitutively phosphorylated serine residue (P-mimic, hyper-P mutation) and may be optimally paired with studies of the isosteric but not charged (hypo-P mutation) mutant using glutamine (Tarrant & Cole, 2009).

Microscopic analyses indicated that the wild-type DsRed-labelled dUTPase (WT DsR-DUT) is mainly nuclear in an asynchronous 293T cell population, whereas the hyper-P S11E mutant is cytoplasmic (Fig. 2). The isosteric control hypo-P S11Q mutant reverts back to nuclear localization, indicating that the introduced negative charge is responsible for the altered localization pattern of the S11E mutant. This behaviour of the WT and mutant dUTPases was confirmed in a number of cell types with diverse genetic backgrounds

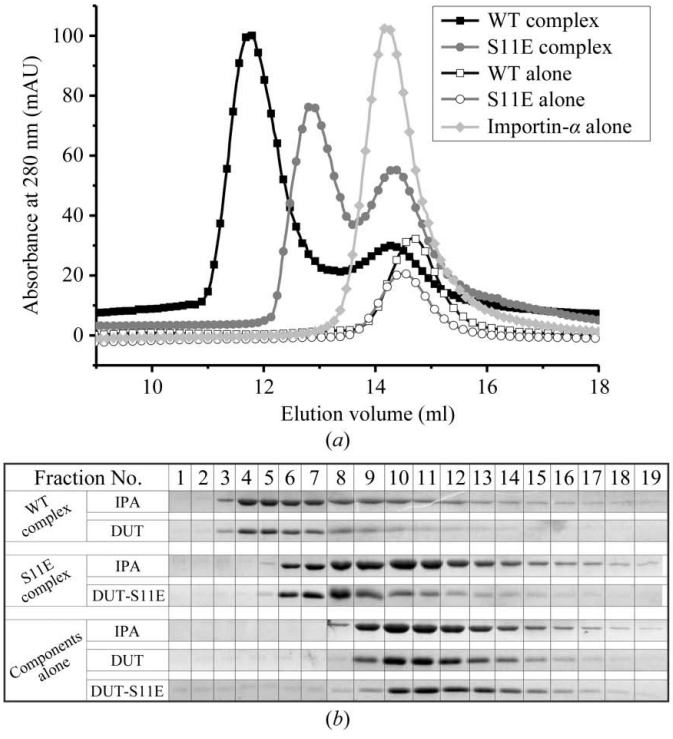


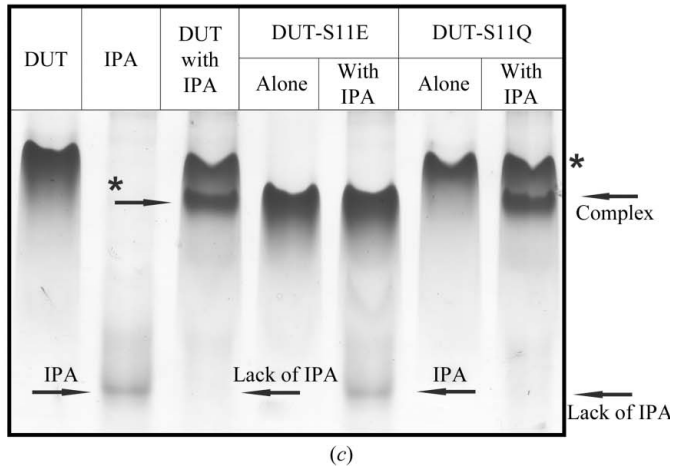


**Figure 3**
dUTPase forms a stable complex with importin-$\alpha$ *in vitro*. (*a*, *b*) Size-exclusion chromatography and (*c*) native gel results showing complex formation between dUTPase and importin-$\alpha$ (IPA) weakened by the S11E mutation. (*a*) Gel-filtration chromatograms. When applied alone, dUTPase and importin-$\alpha$ elute at elution volumes of 14.8 and 14.3 ml, respectively. When applied in a mixture, a new elution peak is observed at an elution volume of 11.6 or 12.8 ml for mixtures of WT dUTPase or S11E mutant dUTPase with importin-$\alpha$, respectively, while some of the protein also elutes at the position corresponding to the free components. These data may suggest that for both WT and S11E mutant dUTPase a complex associated with a higher molecular mass is produced in the presence of importin-$\alpha$; however, this complex is less stable with S11E dUTPase (Beeckmans, 1999). (*b*) Fractions from the gel-filtration chromatography were analyzed by SDS–PAGE. Note that the peaks eluting at the early positions (11.6 and 12.8 ml) in the mixtures contain both dUTPase and importin-$\alpha$, reinforcing the suggestion of complex formation. (*c*) Native gel electrophoretograms. dUTPase (DUT) and importin-$\alpha$ (IPA) were run on native gels either alone or in a mixture, as indicated at the top of the lanes. Arrows with a star and designated as 'complex' at the upper position of the gels indicate the new band that appears in the mixture of either WT or S11Q dUTPase and importin-$\alpha$ but that is not present in the mixture of S11E dUTPase and importin-$\alpha$. When applied alone to the native gel, the S11E dUTPase appears at a lower band position than the WT or S11W dUTPases, probably owing to its extra negative charge. This position is accidentally rather close to the position of the band labelled 'complex' in the mixtures of WT and S11Q dUTPases. However, no new band is observed when S11E dUTPase and importin-$\alpha$ are mixed. Note that in lanes in which this 'complex' band is present, the band for the free uncomplexed importin-$\alpha$ disappears (arrow labelled 'lack of IPA'). whereas this uncomplexed importin-$\alpha$ band is still present in the mixture with S11E dUTPase.

(differing in both the origin and the modes of transformation; Supplementary Fig. S2). The results clearly show that the hyper-P mutation drastically interferes with cellular localization regardless of cell type.

In order to check whether active nuclear export contributed to the strict exclusion of the S11E mutant dUTPase from the nucleus, we used leptomycin B, a well described specific inhibitor of one of the major exportins, CRM1 (Fornerod *et al.*, 1997). Leptomycin B had no effect on the localization of the S11E dUTPase (Supplementary Fig. S3). Therefore, we conclude that the exclusive cytoplasmic localization of the S11E mutant dUTPase construct is probably owing to perturbation of its nuclear import and not of its export.

In summary, we found that dUTPase phosphorylation occurs in the M phase of the cell cycle, supporting the role of Cdk1 kinase. We have also shown that the P-mimicking S11E mutation leads to exclusion from the nucleus. In the next experiments, we wished to determine whether the impeded import results from perturbation of the importin-$\alpha$–dUTPase interaction and also wished to obtain insight into the molecular details of this regulation based on three-dimensional structural data.

### 3.2. Molecular details of the interaction between human dUTPase and importin-$\alpha$

Several independent biophysical methods were used to evaluate the complex formation of WT, hypo-P S11Q and hyper-P S11E mutant dUTPases and importin-$\alpha$ (for the latter protein, a construct lacking the autoinhibitory domain, importin-$\alpha$ $\Delta$IBB, was used throughout the study). Analytical gel filtration showed that in the mixture of WT dUTPase and importin-$\alpha$ a molecular species elutes at a position corresponding to a significantly higher molecular mass than either of the components separately, arguing for a complex formed between the two proteins. A fraction of the protein still elutes at the position corresponding to the free components, potentially representing an uncomplexed fraction (Figs. 3*a* and 3*b*). However, when S11E mutant dUTPase was used the elution behaviour was significantly different, showing a peak that

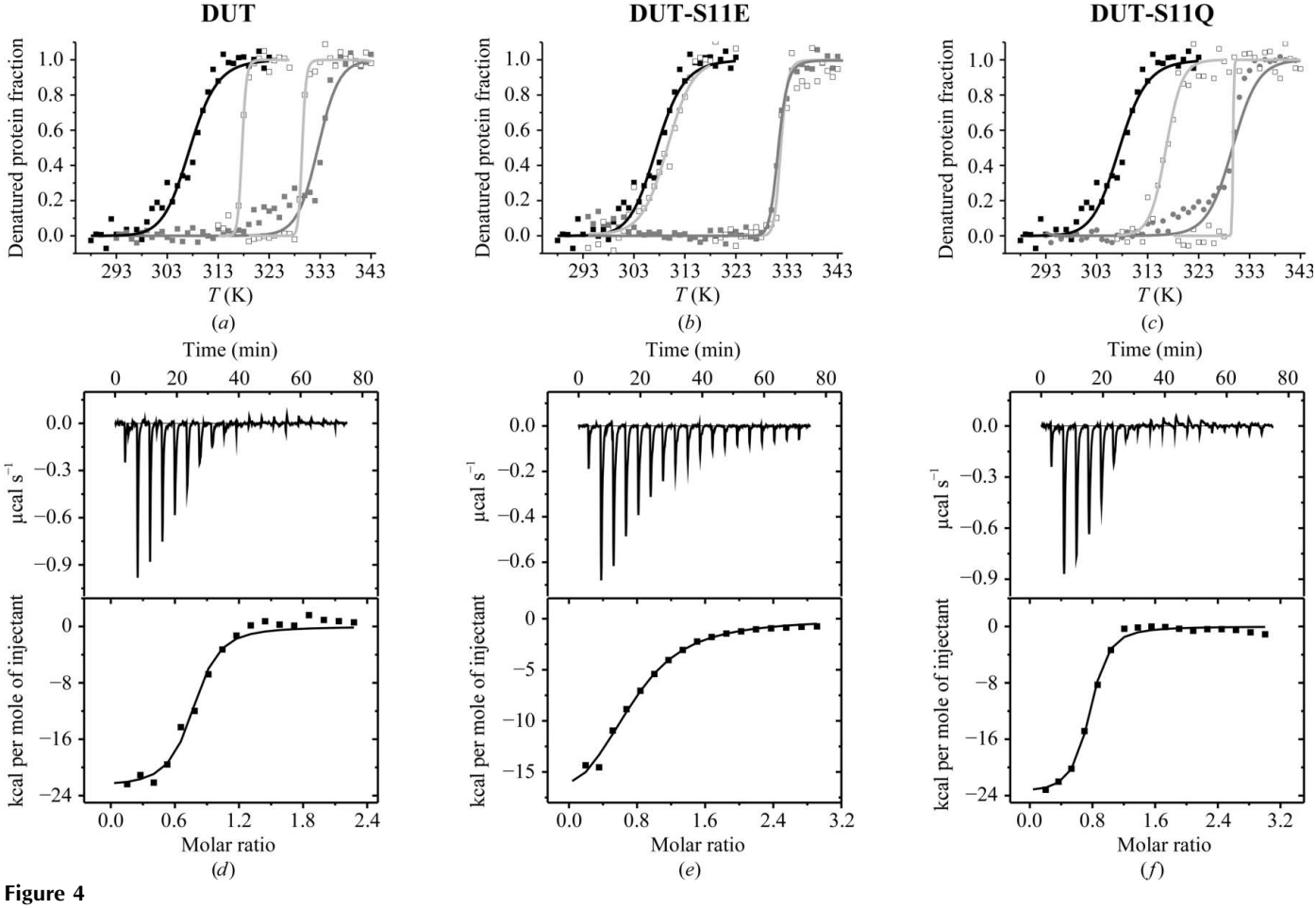


**Figure 4**
Thermodynamic analysis of complex formation between dUTPase and importin-$\alpha$ using circular dichroism at 210 nm during thermal denaturation (*a*, *b*, *c*) and isothermal titration (*d*, *e*, *f*). In the denaturation scans (*a*, *b*, *c*), curves are shown for importin-$\alpha$ (black squares), dUTPase (grey squares) and their mixture (empty squares). In the complex (*a*, *c*) two transitions were observed, presumably reflecting partially separate unfolding events of complexed proteins (Table 2). In isothermal titration (*d*, *e*, *f*) the top panels present the baseline-corrected response for the power compensation of the ITC instrument during titration and the bottom panels show the integrated heat data (black squares) and the fit of the binding isotherm by an 'independent binding sites' model (solid line). (*a*) and (*d*) show data for WT, (*b*) and (*e*) show data for the S11E mutant and (*c*) and (*f*) show data for the S11Q mutant. The values extracted are shown in Table 2.

eluted earlier than any of the components alone but later than the peak tentatively associated with the WT dUTPase–importin-$\alpha$ complex (Figs. 3*a* and 3*b*). Also, the protein fraction eluting at the position corresponding to the free components is larger. This behaviour might be explained by assuming that the complex formed between S11E dUTPase and importin-$\alpha$ is characterized by a faster dynamic equilibrium, *i.e.* it is less stable compared with the WT dUTPase–importin-$\alpha$ complex (for a review of gel-filtration analysis of dynamic and stable protein complexes, see Beeckmans, 1999).

To investigate the complex formation further by additional independent techniques, we used native PAGE (Fig. 3*c*). The results clearly showed that WT dUTPase and importin-$\alpha$ form a complex which appears at a new position on the gels, while the band corresponding to uncomplexed importin-$\alpha$ disappears. The same complex formation could be observed with the S11Q mutant dUTPase and importin-$\alpha$. In contrast, complex formation between the S11E mutant dUTPase and importin-$\alpha$ could not be detected (Fig. 3*c*). The results indicate that the different nucleocytoplasmic localization patterns of the S11E and S11Q mutants are likely to be attributable to modulation of the dUTPase–importin-$\alpha$ interaction: the S11Q mutant forms a stable complex with importin-$\alpha$, whereas the S11E mutant does not.

Complex formation between WT or S11Q mutant dUTPase with importin-$\alpha$ was also confirmed using thermal denaturation experiments of the individual components and their mixtures. Heat-induced unfolding was followed by circular-dichroism spectroscopy. We found that interaction leads to a strong stabilization against heat-induced unfolding and also renders the thermal unfolding transition significantly more cooperative (Figs. 4*a*, 4*b* and 4*c*). We observed this stabilizing effect in mixtures of importin-$\alpha$ with either the WT or S11Q mutant dUTPases, but not with the S11E mutant dUTPase (Table 2). These results again reinforced the previous conclusion that the P-mimicking negative charge (S11E) impedes complex formation, whereas the isosteric control glutamine mutant (S11Q) has the same capability to bind to importin-$\alpha$ as the WT protein.

For a direct quantitative analysis of the effect of phosphorylation on complex formation, we performed isothermal titration microcalorimetry (ITC) assays (Figs. 4*d*, 4*e* and 4*f*). The S11E mutation increased the dissociation constant of the complex by approximately one order of magnitude (the $K_{\rm d}$ values were 0.79, 0.76 and 9.62 $\mu M$ for the WT, S11Q and S11E dUTPases, respectively; Table 2). The determined stoichiometry is in agreement with a model in which each NLS of the trimeric dUTPase cargo binds one importin-$\alpha$ molecule, consistent with the case for the pentameric nucleoplasmin cargo protein (Falces *et al.*, 2010).

To characterize the three-dimensional structural basis of the interaction, we determined the crystal structures of importin-$\alpha$ in complex with peptides corresponding to the WT (PDB entry 4mz5) and S11E (PDB entry 4mz6) NLSs (Figs. 5 and 6; stereoviews are shown in Supplementary Figs. S4 and S5, respectively). In the electron-density maps both NLS peptides are present with clearly well defined densities in the major binding site of importin-$\alpha$. Lys14 of the dUTPase peptides forms a salt bridge to Asp192 of importin-$\alpha$, analogous to all previously deposited three-dimensional structures of importin-$\alpha$–NLS (Marfori *et al.*, 2011). The S11E P-mimic mutation does not lead to a major conformational change in the complex structure; even the C-terminal segment of the NLS peptide is able to use the same coordination environment within the complex. However, in this mutant the introduced Glu side chain creates an intra-NLS contact with Arg15 of the human dUTPase NLS, thereby flipping the Arg15 side chain in the P3 binding pocket into an alternative position in which it loses contact with the importin-$\alpha$ Asn228 side chain (Fig. 6). Notably, this conformational shift creates a salt-bridge interaction between Arg15 of the dUTPase NLS and Asp270 of importin-$\alpha$. Both Arg15 of the cargo protein and Asn228 of importin-$\alpha$ are strongly conserved in the respective proteins. In this flipped conformation, the highly conserved importin-$\alpha$ side chains of Trp231, Trp273 and Arg238 undergo slight conformational changes in their side-chain positions to accommodate the Arg15–Asp270 interaction. More significantly, the main chain of the residues N-terminal to the P2 Lys now follows a different trajectory to that in the WT peptide (Fig. 6*c*). This results in a loss of hydrogen bonds between Pro12 of the P-mimic peptide and the importin-$\alpha$ surface. In summary, the P-mimic Glu mutation at the Ser11 position induces an alternative conformation of Arg15 of the human dUTPase NLS and this leads to a rearrangement of the accommodation pattern of the peptide in the importin-$\alpha$ binding site. This rearrangement results in the loss of interactions between the Pro12, Arg15 NLS residues and the importin-$\alpha$ surface, thus explaining the weaker binding of the

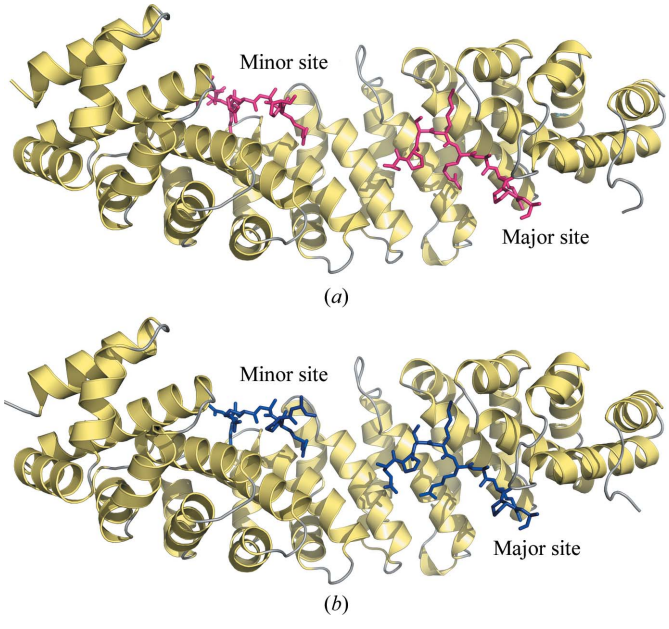


**Figure 5**
Structural basis of the effect of phosphorylation adjacent to NLSs on binding: crystal structures of importin-$\alpha$ ΔIBB (yellow cartoon) in complex with dUTPase WT NLS peptide (*a*) and dUTPase S11E P-mimic NLS peptide (*b*) (hot pink and blue sticks, respectively).

P-mimic S11E mutant dUTPase to importin-$\alpha$ shown in the solution experiments.

## 4. Conclusions

Here, we have shown that NLS-adjacent phosphorylation of human dUTPase results in cytoplasmic accumulation of the otherwise nuclear enzyme in a large number of cell types, including spontaneously transformed cells and tumour cells of different origins.

Our *in vitro* biophysical investigations indicated that the formation of a complex between a cargo protein NLS and the nuclear transport factor importin-$\alpha$ is significantly weakened by the introduction of a P-mimicking negatively charged residue at the P−1 position of the NLS. The dissociation constant of the cargo protein–importin complex decreased by one order of magnitude and this decrease led to complete abolition of nuclear import of the cargo. The 2.1 Å resolution crystal structure of the dUTPase peptide–importin-$\alpha$ complex clearly delineates the atomic interactions that are responsible for complex formation and provides detailed insights into the mechanism responsible for perturbation of this connection.

Having described the molecular details of the dUTPase–importin-$\alpha$ complexes, we were interested in the potential general implications of our findings. Phosphorylation adjacent to the NLS resulting in inhibition of nuclear transport has previously been reported in the case of several proteins (Table 1 and references therein). In many cases, Cdk1 or the yeast orthologue Cdc28 have been proposed to be responsible for the phosphorylation event, which takes place at the P0 or

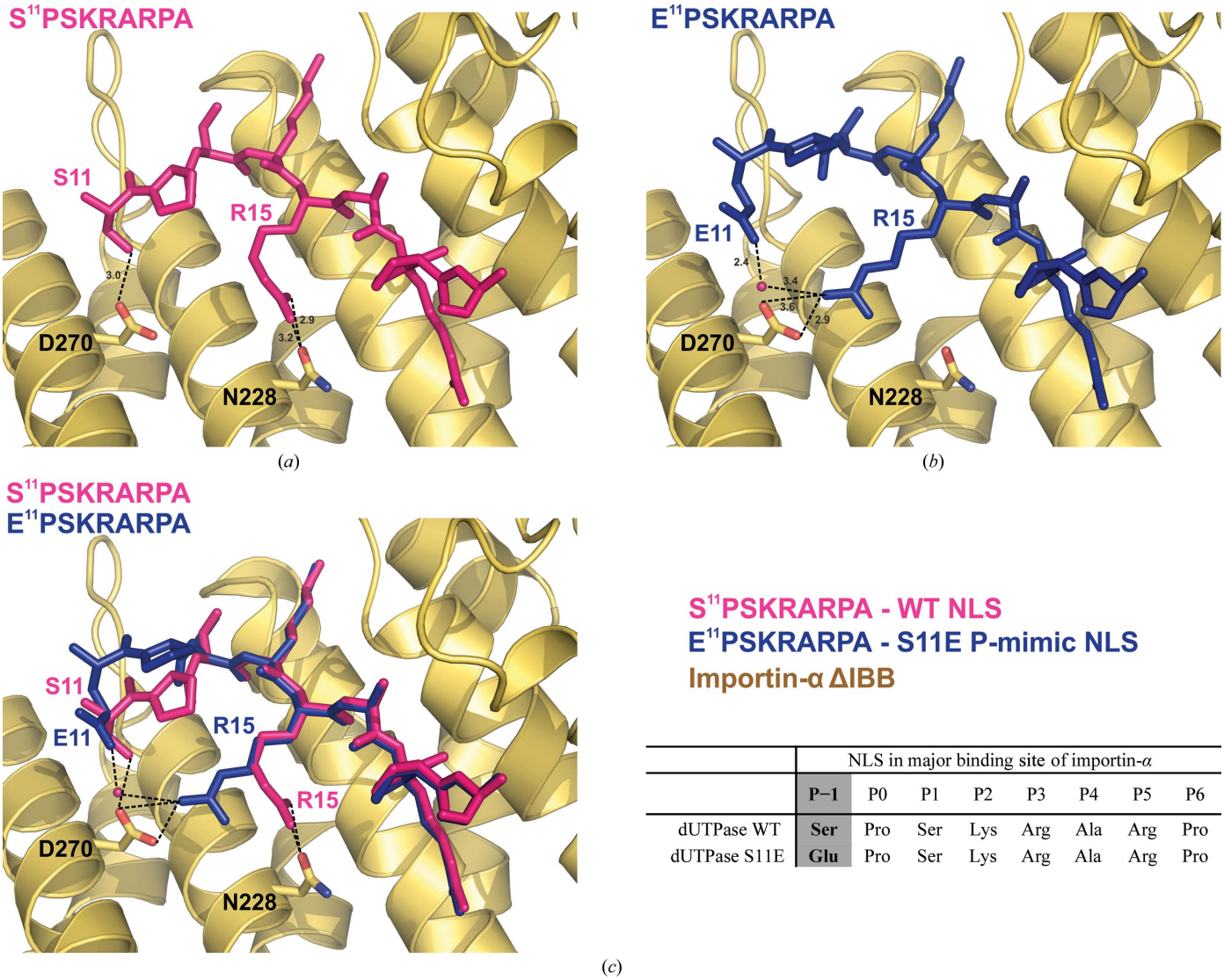


| | NLS in major binding site of importin-$\alpha$ | | | | | | | |
|---|---|---|---|---|---|---|---|---|
| | **P−1** | P0 | P1 | P2 | P3 | P4 | P5 | P6 |
| dUTPase WT | **Ser** | Pro | Ser | Lys | Arg | Ala | Arg | Pro |
| dUTPase S11E | **Glu** | Pro | Ser | Lys | Arg | Ala | Arg | Pro |

**Figure 6**
Close-up views of the interactions of wild-type and mutant NLS segments with importin-$\alpha$ ΔIBB. (*a*) Close-up views of the interactions of WT dUTPase NLS (left) and (*b*) S11E P-mimic NLS. The dUTPase Arg15 side chain interacts with Asn228 in the case of the wild-type peptide, but forms alternative interactions with Asp270 in the S11E P-mimic NLS peptide (Asn228 and Asp270 are shown in stick representation). (*c*) Superimposition of importin-$\alpha$–WT dUTPase and importin-$\alpha$–S11E dUTPase NLS complexes, showing the different main-chain trajectories of the NLS peptides N-terminal to the P1 position.

P−1 position. The described effects of phosphorylation are similar to the effect of Cdk1-mediated phosphorylation at the P−1 position of the dUTPase NLS (Fig. 6). Therefore, we propose that the crystallographic model presented in our study sheds light on a general structural mechanism that lies behind the phosphorylation-mediated inhibition of nuclear import.

This work was supported by the Hungarian Scientific Research Fund (OTKA NK 84008, PD72008, OTKA K 109486), the Baross program of the New Hungary Development Plan (3DSTRUCT, OMFB-00266/2010 REG-KM-09-1-2009-0050), the Hungarian Academy of Sciences (TTK IF-28/2012) and the European Commission FP7 BioStruct-X project (contract No. 283570). This work was also supported by a Lendület grant from the Hungarian Academy of Sciences (LB). JT is the recipient of the János Bolyai Research Scholarship of the Hungarian Academy of Sciences. BK is a National Health and Medical Research Council Research Fellow.

## References

Adams, P. D. *et al.* (2010). *Acta Cryst.* D**66**, 213–221.
Beeckmans, S. (1999). *Methods*, **19**, 278–305.
Békési, A., Zagyva, I., Hunyadi-Gulyás, E., Pongrácz, V., Kovári, J., Nagy, A. O., Erdei, A., Medzihradszky, K. F. & Vértessy, B. G. (2004). *J. Biol. Chem.* **279**, 22362–22370.
Bozóky, Z., Róna, G., Klement, É., Medzihradszky, K. F., Merényi, G., Vértessy, B. G. & Friedrich, P. (2011). *PLoS One*, **6**, e19546.
Chen, V. B., Arendall, W. B., Headd, J. J., Keedy, D. A., Immormino, R. M., Kapral, G. J., Murray, L. W., Richardson, J. S. & Richardson, D. C. (2010). *Acta Cryst.* D**66**, 12–21.
Cowtan, K., Emsley, P. & Wilson, K. S. (2011). *Acta Cryst.* D**67**, 233–234.
Duncan, B. K. & Weiss, B. (1982). *J. Bacteriol.* **151**, 750–755.
Emsley, P. & Cowtan, K. (2004). *Acta Cryst.* D**60**, 2126–2132.
Enquist-Newman, M., Sullivan, M. & Morgan, D. O. (2008). *Mol. Cell*, **30**, 437–446.
Falces, J., Arregi, I., Konarev, P. V., Urbaneja, M. A., Svergun, D. I., Taneva, S. G. & Bañuelos, S. (2010). *Biochemistry*, **49**, 9756–9769.
Fontes, M. R., Teh, T., Jans, D., Brinkworth, R. I. & Kobe, B. (2003). *J. Biol. Chem.* **278**, 27981–27987.
Fontes, M. R., Teh, T. & Kobe, B. (2000). *J. Mol. Biol.* **297**, 1183–1194.
Fontes, M. R., Teh, T., Toth, G., John, A., Pavo, I., Jans, D. A. & Kobe, B. (2003). *Biochem. J.* **375**, 339–349.
Fornerod, M., Ohno, M., Yoshida, M. & Mattaj, I. W. (1997). *Cell*, **90**, 1051–1060.
Gadsden, M. H., McIntosh, E. M., Game, J. C., Wilson, P. J. & Haynes, R. H. (1993). *EMBO J.* **12**, 4425–4431.
Galperin, M. Y., Moroz, O. V., Wilson, K. S. & Murzin, A. G. (2006). *Mol. Microbiol.* **59**, 5–19.
Geymonat, M., Spanos, A., Wells, G. P., Smerdon, S. J. & Sedgwick, S. G. (2004). *Mol. Cell. Biol.* **24**, 2277–2285.
Görlich, D., Vogel, F., Mills, A. D., Hartmann, E. & Laskey, R. A. (1995). *Nature (London)*, **377**, 246–248.
Hagen, L., Kavli, B., Sousa, M. M., Torseth, K., Liabakk, N. B., Sundheim, O., Pena-Diaz, J., Otterlei, M., Hørning, O., Jensen, O. N., Krokan, H. E. & Slupphaug, G. (2008). *EMBO J.* **27**, 51–61.
Harreman, M. T., Kline, T. M., Milford, H. G., Harben, M. B., Hodel, A. E. & Corbett, A. H. (2004). *J. Biol. Chem.* **279**, 20613–20621.
Hennekes, H., Peter, M., Weber, K. & Nigg, E. A. (1993). *J. Cell Biol.* **120**, 1293–1304.
Huynh, M. A., Stegmüller, J., Litterman, N. & Bonni, A. (2009). *J. Neurosci.* **29**, 4322–4327.
Ikuta, T., Kobayashi, Y. & Kawajiri, K. (2004). *Biochem. Biophys. Res. Commun.* **317**, 545–550.
Jans, D. A., Ackermann, M. J., Bischoff, J. R., Beach, D. H. & Peters, R. (1991). *J. Cell Biol.* **115**, 1203–1212.
Jans, D. A. & Hübner, S. (1996). *Physiol. Rev.* **76**, 651–685.
Jans, D. A., Moll, T., Nasmyth, K. & Jans, P. (1995). *J. Biol. Chem.* **270**, 17064–17067.
Jaquenoud, M., van Drogen, F. & Peter, M. (2002). *EMBO J.* **21**, 6515–6526.
Kabsch, W. (2010). *Acta Cryst.* D**66**, 125–132.
Kaffman, A., Rank, N. M. & O'Shea, E. K. (1998). *Genes Dev.* **12**, 2673–2683.
Koehler, S. E. & Ladner, R. D. (2004). *Mol. Pharmacol.* **66**, 620–626.
Kosugi, S., Hasebe, M., Tomita, M. & Yanagawa, H. (2009). *Proc. Natl Acad. Sci. USA*, **106**, 10171–10176.
Kovári, J., Barabás, O., Varga, B., Békési, A., Tölgyesi, F., Fidy, J., Nagy, J. & Vértessy, B. G. (2008). *Proteins*, **71**, 308–319.
Ladner, R. D. & Caradonna, S. J. (1997). *J. Biol. Chem.* **272**, 19072–19080.
Ladner, R. D., Carr, S. A., Huddleston, M. J., McNulty, D. E. & Caradonna, S. J. (1996). *J. Biol. Chem.* **271**, 7752–7757.
Ladner, R. D., McNulty, D. E., Carr, S. A., Roberts, G. D. & Caradonna, S. J. (1996). *J. Biol. Chem.* **271**, 7745–7751.
Lange, A., Mills, R. E., Lange, C. J., Stewart, M., Devine, S. E. & Corbett, A. H. (2007). *J. Biol. Chem.* **282**, 5101–5105.
Lee, M. K., Tong, W. M., Wang, Z. Q. & Sabapathy, K. (2010). *Cell Death Differ.* **18**, 214–221.
Liku, M. E., Nguyen, V. Q., Rosales, A. W., Irie, K. & Li, J. J. (2005). *Mol. Biol. Cell*, **16**, 5026–5039.
MacFarlane, A. J., Anderson, D. D., Flodby, P., Perry, C. A., Allen, R. H., Stabler, S. P. & Stover, P. J. (2011). *J. Biol. Chem.* **286**, 44015–44022.
Marfori, M., Lonhienne, T. G., Forwood, J. K. & Kobe, B. (2012). *Traffic*, **13**, 532–548.
Marfori, M., Mynott, A., Ellis, J. J., Mehdi, A. M., Saunders, N. F., Curmi, P. M., Forwood, J. K., Bodén, M. & Kobe, B. (2011). *Biochim. Biophys. Acta*, **1813**, 1562–1577.
McCoy, A. J., Grosse-Kunstleve, R. W., Adams, P. D., Winn, M. D., Storoni, L. C. & Read, R. J. (2007). *J. Appl. Cryst.* **40**, 658–674.
McPhillips, T. M., McPhillips, S. E., Chiu, H.-J., Cohen, A. E., Deacon, A. M., Ellis, P. J., Garman, E., Gonzalez, A., Sauter, N. K., Phizackerley, R. P., Soltis, S. M. & Kuhn, P. (2002). *J. Synchrotron Rad.* **9**, 401–406.
Merényi, G., Kovári, J., Tóth, J., Takács, E., Zagyva, I., Erdei, A. & Vértessy, B. G. (2011). *Nucleosides Nucleotides Nucleic Acids*, **30**, 369–390.
Mol, C. D., Harris, J. M., McIntosh, E. M. & Tainer, J. A. (1996). *Structure*, **4**, 1077–1092.
Moll, T., Tebb, G., Surana, U., Robitsch, H. & Nasmyth, K. (1991). *Cell*, **66**, 743–758.
Muha, V., Horváth, A., Békési, A., Pukáncsik, M., Hodoscsek, B., Merényi, G., Róna, G., Batki, J., Kiss, I., Jankovics, F., Vilmos, P., Erdélyi, M. & Vértessy, B. G. (2012). *PLoS Genet.* **8**, e1002738.
Muha, V., Zagyva, I., Venkei, Z., Szabad, J. & Vértessy, B. G. (2009). *Biochem. Biophys. Res. Commun.* **381**, 271–275.
Nagy, G. N., Marton, L., Krámos, B., Oláh, J., Révész, A., Vékey, K., Delsuc, F., Hunyadi-Gulyás, É., Medzihradszky, K. F., Lavigne, M., Vial, H., Cerdan, R. & Vértessy, B. G. (2013). *FEBS J.* **280**, 3132–3148.
Nardozzi, J. D., Lott, K. & Cingolani, G. (2010). *Cell Commun. Signal.* **8**, 32.
Németh-Pongrácz, V., Barabás, O., Fuxreiter, M., Simon, I., Pichová, I., Rumlová, M., Zábranská, H., Svergun, D., Petoukhov, M., Harmat, V., Klement, E., Hunyadi-Gulyás, E., Medzihradszky, K. F., Kónya, E. & Vértessy, B. G. (2007). *Nucleic Acids Res.* **35**, 495–505.
Pecsi, I., Hirmondo, R., Brown, A. C., Lopata, A., Parish, T., Vertessy, B. G. & Tóth, J. (2012). *PLoS One*, **7**, e37461.

Pecsi, I., Leveles, I., Harmat, V., Vertessy, B. G. & Toth, J. (2010). *Nucleic Acids Res.* **38**, 7179–7186.
Pécsi, I., Szabó, J. E., Adams, S. D., Simon, I., Sellers, J. R., Vértessy, B. G. & Tóth, J. (2011). *Proc. Natl Acad. Sci. USA*, **108**, 14437–14442.
Poon, I. K. & Jans, D. A. (2005). *Traffic*, **6**, 173–186.
Sidorova, J. M., Mikesell, G. E. & Breeden, L. L. (1995). *Mol. Biol. Cell*, **6**, 1641–1658.
Stephen, A. G., Trausch-Azar, J. S., Handley-Gearhart, P. M., Ciechanover, A. & Schwartz, A. L. (1997). *J. Biol. Chem.* **272**, 10895–10903.
Tagawa, T., Kuroki, T., Vogt, P. K. & Chida, K. (1995). *J. Cell Biol.* **130**, 255–263.
Takács, E., Barabás, O., Petoukhov, M. V., Svergun, D. I. & Vértessy, B. G. (2009). *FEBS Lett.* **583**, 865–871.
Takács, E., Grolmusz, V. K. & Vértessy, B. G. (2004). *FEBS Lett.* **566**, 48–54.
Tarrant, M. K. & Cole, P. A. (2009). *Annu. Rev. Biochem.* **78**, 797–825.
Tinkelenberg, B. A., Fazzone, W., Lynch, F. J. & Ladner, R. D. (2003). *Exp. Cell Res.* **287**, 39–46.
Tóth, J., Varga, B., Kovács, M., Málnási-Csizmadia, A. & Vértessy, B. G. (2007). *J. Biol. Chem.* **282**, 33572–33582.
Varga, B., Barabás, O., Kovári, J., Tóth, J., Hunyadi-Gulyás, E., Klement, E., Medzihradszky, K. F., Tölgyesi, F., Fidy, J. & Vértessy, B. G. (2007). *FEBS Lett.* **581**, 4783–4788.
Vértessy, B. G. & Tóth, J. (2009). *Acc. Chem. Res.* **42**, 97–106.
Winn, M. D. *et al.* (2011). *Acta Cryst.* D**67**, 235–242.
Zhou, Y., Ching, Y.-P., Chun, A. C. S. & Jin, D.-Y. (2003). *J. Biol. Chem.* **278**, 12530–12536.